Wang, M., Lin, C.-H., and Chen, Q. 2012. "Advanced turbulence models for predicting particle transport in enclosed environment," **Building and Environment,** 47, 40-49.

Advanced Turbulence Models for Predicting Particle Transport in Enclosed Environments

Miao Wang[1], Chao-Hsin Lin[2] and Qingyan Chen[1]
[1]School of Mechanical Engineering, Purdue University, West Lafayette, IN 47907, USA
[2]2Environmental Control Systems, Boeing Commercial Airplanes, Everett, WA 98124, USA
Phone: (765) 496-7562, FAX: (765) 496-0539, Email: yanchen@purdue.edu

Abstract

Occupant health is related to particle contaminants in enclosed environments, so it is important to study particle transport in spaces to quantify the rates and routes of potential disease transmission. In many cases, particle contaminants in an enclosed space are generated from an unsteady source. This investigation used the experimental data from two steady-state cases as well as one transient particle dispersion case in evaluating the performance of five (one steady and four transient) airflow models with the Eulerian and Lagrangian methods. The transient models obtained the mean flow and particle information by averaging them over time. For the models tested in this study, the Eulerian method performed similarly for all five airflow models. The Lagrangian method predicted incorrect particle concentrations with the Reynolds-Averaged Navier-Stokes (RANS) and Unsteady Reynolds-Averaged Navier-Stokes (URANS) methods, but did well with the Large Eddy Simulation (LES) and Detached Eddy Simulation (DES) models. For unsteady-state particle dispersion, the LES or DES models, along with the Lagrangian method, showed the best performance among all the models tested.

1. Introduction

The level of airborne particle concentration in enclosed environments is an important factor in indoor air quality as well as the quantification of the rates and routes of potential disease transmission. Exposure to airborne particles has been shown to be closely related to adverse health effects, such as respiratory and cardiovascular diseases, asthma attacks, and cardiac arrhythmia [1]. Moreover, infectious disease transmission in vehicle cabins has become one of the main health concerns in the world. Particularly in commercial aircraft where occupants are in close proximity, virus laden bio-aerosols generated by infected occupants through coughing or sneezing can be transmitted throughout the cabin and can infect other occupants [2-4].

In order to understand the route of airborne contaminant transportation; to assess the risk of airborne diseases, micro-organic, and chemical agents; and to reduce the level of contaminant concentration, it is essential to accurately model the particle transportation processes in enclosed spaces. Since the aerosol particles are suspended and dispersed in

the surrounding airflow, the airflow motion in the enclosed spaces should be correctly modeled. As a powerful airflow modeling tool, Computational Fluid Dynamics (CFD) can be applied to simulate the airflow field and provide a particle model with flow information, such as recirculation patterns, temperature distribution, and turbulence eddy structure. Using this information, the particle model can be employed to simulate the particle transport processes and evaluate the spatial and temporal particle contaminant distributions.

The particle transport processes can be in both steady and unsteady states. For the steady-state cases, particle contaminants are released from particle source(s) at a constant rate, while the surrounding airflow field does not change with time. Since it is easy to measure the averaged particle concentration, many experimental and numerical investigations have been conducted on steady-state particle transportation in enclosed environments. For example, Murakami et al. [5] studied the diffusion characteristics of airborne particles in a clean room, and Zhang and Chen [6] measured and simulated a room with an Under-Floor Air Distribution (UFAD) system with two particle sources. Zhang et al. [7] also investigated airflow and particulate contaminant transport in a four-row airline cabin mockup. Yin et al. [8] studied particles released by an infected patient in a patient ward. In most of these studies, a steady-state RANS model was used along with either an Eulerian or a Lagrangian particle model, which predicted reasonable contaminant concentration distributions.

Although the steady-state particle transportation process may be simulated, the assumptions of the constant release of particles and steady-state airflow field only hold in a few cases. In most cases, particle transport processes are in unsteady-state. In a steady-state airflow field, the particle concentration can be time-dependent. For example, contaminant particles can accumulate in an indoor environment with constant ventilation rate. In this case, either a steady-state or an unsteady-state airflow model can be used to provide unsteady-state particle model with airflow information. The time-dependent particle field can also be found with unsteady-state airflow. For example, particle transport due to moving object or the presence of human beings in the indoor environment can be transient. In this case, an unsteady airflow model should be applied along with a particle transport model. In the literature, unsteady-state airflow models such as LES and DES have been used by many studies to simulate airflow in enclosed spaces [9-11]. These models have shown good performance and have been widely applied in indoor airflow modeling [12-14]. However, the difficulties in measuring an unsteady particle concentration field make it hard to evaluate the model performance. A few studies from the literature have conducted unsteady particle simulations. For example, the study by Zhang and Chen [7] tested the Eulerian and Lagrangian methods with an unsteady RNG k-ε model by simulating a cough in a four-row airliner cabin. They found that the Eulerian method predicted unrealistic particle concentration distribution in an unsteady state. However, the transient particle concentration field from the Lagrangian method could not be verified.

This paper reports our effort in evaluating the performance of unsteady airflow models with the Eulerian and Lagrangian methods by experimental data. Due to the lack of high

quality experimental data for unsteady particle dispersion, two cases still used steady-state and one used unsteady-state. For the steady-state cases, the unsteady airflow and particle models were used in a transient manner, i.e., calculating the transient flow and particle concentration field over a period of time. The transient results were averaged over that period, and the mean values were compared with the experimental data. Our investigation was to identify a suitable model for predicting different airflow and particle transportation in enclosed environments.

2. Airflow and particle contaminant models

This section introduces five popular airflow models and two particle simulation methods. Due to the limited space available in this paper, the focus was on the model properties and their impact on the resolved particle transportation.

2.1. Modeling airflow

2.1.1. RANS

The most popular turbulence model for steady-state airflow and contaminant transport simulation in enclosed environments is Reynolds-Averaged Navier-Stokes equation (RANS) modeling. This model separates an instantaneous variable, $\phi\left(\vec{x}\right)$, into a mean $\overline{\phi}\left(\vec{x}\right)$ component and a fluctuating component, $\phi'\left(\vec{x}\right)$:

$$\phi\left(\vec{x}\right)=\overline{\phi}\left(\vec{x}\right)+\phi'\left(\vec{x}\right) \tag{2.1}$$

The mean value of the flow variables is defined as:

$$\overline{\phi}\left(\vec{x}\right)=\lim_{T\to\infty}\frac{1}{T}\int_0^T\phi\left(\vec{x},t\right)dt \tag{2.2}$$

As a result, the continuity and the Navier-Stokes equation for incompressible flow can be written as:

$$\frac{\partial\overline{u_i}}{\partial x_i}=0 \tag{2.3}$$

$$\overline{u}_j\frac{\partial\overline{u_i}}{\partial x_j}=-\frac{1}{\rho}\frac{\partial\overline{P}}{\partial x_i}+\nu\frac{\partial^2\overline{u}_i}{\partial x_j\partial x_j}+\frac{\partial\tau_{ij}}{\partial x_j} \tag{2.4}$$

where u_i and x_i are the air velocity and coordinate in the i direction respectively, P is the air pressure. The over bar denotes the mean variables. The term τ_{ij} is the Reynolds stresses and should be modeled to complete the closure.

Various RANS turbulence models have been developed in the last four decades, many of which have been used for indoor airflow simulations. Comparative studies showed that the RNG k-ε model had the best overall performance among all RANS models for enclosed environments [10, 11]. Therefore, the RNG k-ε model was used in this investigation. Due to the limited space available in this paper, the equations for the RNG k-ε model were not provided but they can be found in reference [15].

2.1.2. Unsteady-RANS

For unsteady airflow, the URANS method can easily be derived from the steady RANS to solve the time-dependent flow. Similar to a RANS model, the URANS separates a flow variable into:

$$\phi\left(\vec{x},t\right)=\overline{\phi}\left(\vec{x},t\right)+\phi'\left(\vec{x},t\right) \tag{2.5}$$

where $\phi'\left(\vec{x},t\right)$ is the fluctuating part of the flow variables and $\overline{\phi}\left(\vec{x},t\right)$ is the mean value of the flow variables, which is defined as:

$$\overline{\phi}\left(\vec{x},t\right)=\frac{1}{T}\int_{t}^{t+T}\phi\left(\vec{x},t\right)dt \tag{2.6}$$

where T is a time scale that is much larger than the time scale of the turbulence fluctuation, but much smaller than the time scale of the flow variations. As a result, the URANS model has the same continuity equation as RANS, but an additional transient term in the momentum equations:

$$\frac{\partial\overline{u_i}}{\partial t}+\overline{u_j}\frac{\partial\overline{u_i}}{\partial x_j}=-\frac{1}{\rho}\frac{\partial\overline{P}}{\partial x_i}+\nu\frac{\partial^2\overline{u_i}}{\partial x_j\partial x_j}+\frac{\partial\tau_{ij}}{\partial x_j} \tag{2.7}$$

Since the flow variables are averaged over time scale T, which is larger than the turbulence scale, the flow field solved by the URANS model does not contain any turbulence fluctuation. However, these fluctuations could be important for the particle dispersion process. When performing particle dispersion simulation with such a flow field, the turbulence dispersion needs to be modeled correctly.

In contrast to the wide applications of the RANS models, only a few studies can be found in the literature where the URANS models were used to calculate room airflow [16, 17]. Due to the difficulties in measuring unsteady flow, few studies have been performed to validate different URANS models. However, among the few URANS models applied to airflows in enclosed environments, the RNG k-ε model has been the most popular and, hence, is used in the present study [10,11].

2.1.3. Large eddy simulation

During the past decade, LES has become more popular for airflow simulations in enclosed environments [9]. The LES assumes that the turbulence eddies can be separated into large-scale and small-scale eddies. The large-scale eddies are directly affected by the boundary conditions and must be solved. For particle dispersion, the large eddies account for most impacts on particle motions. In contrast, the isotropic small-scale eddies are more universal, and thus more amenable to modeling. As a result, the resolved flow field with large scale eddies by LES is three-dimensional and time-dependent. The particle dispersion due to turbulence motions can be reconstructed by a well-resolved LES flow field. Note that the length scale of the isotropic eddies is much smaller as approaching the solid wall. Therefore the LES requires much finer grid in the near-wall region.

Mathematically, the LES filters the flow variables to keep the large-scale flow motions by applying a filtering operation:

$$\tilde{\phi}(\vec{x},t) = \iiint_V \phi(\vec{x},t) G(\vec{x},\vec{x}',t) d\vec{x}' \tag{2.8}$$

where the tilde denotes the filtered variables, and G is a filter function. The continuity and Navier-Stoke equations have the same form as Equations (2.3) and (2.7) except that the over bar denotes the filtered variable, and the term τ_{ij} is the subgrid-scale stresses due to the filtering process. This term represents the motion of the small-scale eddies and needs to be modeled by a subgrid-scale model. This study used a dynamic Smagorinsky subgrid-scale model, which had a good accuracy and stability in some benchmark studies [10, 11]. The detailed formulation of this model can be found in the literature [18, 19].

2.1.4. Detached eddy simulation

Since the LES requires a very fine grid near a solid wall, the computation cost can be very high for wall bounded flows. To reduce the computational cost, DES has been proposed in the past decade. The DES applies LES in the separated flow region to capture the structure of the unsteady eddies and to apply a RANS model in the attached boundary layers so as to avoid the excessively fine meshes required by LES. Therefore, the airflow resolved by the DES is a combination of filtered time-dependent flow from LES in the mainstream region and time-averaged flow from RANS in the attached boundary layers. For particle dispersion, the DES flow field can reproduce most particle turbulence motions in its LES region, but shares the same drawbacks as the URANS model in the attached boundary layers.

Mathematically, the DES has the same form of continuity and momentum equations as the URANS and LES, as shown in Equations (2.3) and (2.7), respectively. The over bar denotes the mean variables for the RANS and the filtered variables for the LES. The term τ_{ij} in the equation is the Reynolds stresses for the RANS and the subgrid-scale stresses for the LES, which need to be calculated by a DES model. In this paper, two DES models, the DES realizable k-ε (DES1) model and the semi-v2f/LES (DES2) model, were tested. The DES1 model was used due to its good performance in predicting turbulence kinetic energy for typical indoor airflows [11]. This model uses two transport equations for k and

ε. The k is the subgrid-scale turbulence kinetic energy in the LES region and the total kinetic energy in the RANS region. The DES2 model calculates an algebraic equation for wall normal stress v^2 in addition to the k and ε transport equations, which produce a better turbulence viscosity formulation near the wall. The detailed formulation of these two models can be found in the literature [20, 21].

2.2. Modeling particle dispersion

2.2.1. The Eulerian method

The Eulerian method is usually applied for small and dilute particles, whose relaxation time is usually small. The particle can follow the small motions of the flow. The Eulerian method assumes the particle phase to be a continuum which follows the scalar transport equation:

$$\frac{\partial \rho C}{\partial t} + \nabla \cdot \left[\left(\vec{u} + \vec{v}_S \right) \rho C \right] = \nabla \cdot \left(\Gamma \nabla C \right) + S_C \tag{2.9}$$

where t is time, C is the particle concentration; ρ is the air density; $\vec{u}$ is the averaged air velocity components for the RANS models and filtered air velocity components for LES in the three directions; Γ is the effective diffusivity for a particle; $\vec{v}_s$ is the particle settling velocity; and S_c is the particle source term. The particle settling velocity should be modeled to account for mechanisms such as gravitational settling, thermophoresis and electrostatics forces. For the particle size and ventilation arrangement studied in this paper, the dispersion property was similar to those with zero settling velocity [5]. Therefore, $\vec{v}_s$ was set to zero in this study.

The effective particle diffusivity has the form:

$$\Gamma = \rho(\nu_p + D) \tag{2.10}$$

where D is the Brownian diffusivity of particles, which is negligible for a particle in enclosed environments and ν_p is the particle turbulent diffusion coefficient. When the Stokes number of a particle approaches zero, this term equals the turbulence viscosity ν_t for RANS or the subgrid-scale turbulence viscosity for LES [22, 23].

The Eulerian scalar transport equation is solved with the continuity, momentum, turbulence, and energy equations through one-way coupling; i.e., it has no impact on the flow equations. The Eulerian model can easily be applied with all kinds of airflow models in both steady and unsteady states.

2.2.2. The Lagrangian method

Instead of treating particles as a continuum, the Lagrangian method calculates the motion of a large number of individual particles and obtains their trajectories. Therefore, the

Lagrangian method can directly accommodate the physical phenomena of particles, such as forces, heat and mass transfer, chemical reactions, coagulation, and deposition.

For particles in enclosed environments, the particle motion is governed by:

$$\frac{d\vec{u}_p}{dt} = F_D\left(\vec{u} - \vec{u}_p\right) + \frac{\vec{g}\left(\rho_p - \rho\right)}{\rho_p} + \vec{F} \tag{2.11}$$

where, $\vec{u}_p$ and $\vec{u}$ are the particle and air velocities, respectively; ρ_p and ρ are the particle and air densities, respectively; $\vec{g}$ is the gravitational force; $\vec{F}$ is additional forces such as Saffman lift force and Brownian force; and F_D is the drag coefficient. Due to the limited space available in this paper, the formulations of $\vec{F}$ and F_D are not included but can be found in the literature [20].

Note that in Equation (2.11), term $\vec{u}$ is the actual air velocity that should be provided by the airflow model. For the RANS and URANS models, the velocity can be written as:

$$\vec{u} = \bar{u} + u'$$

The mean velocity $\bar{u}$ is solved by the RANS and URANS models. The fluctuating velocity component u' can be calculated by the Discrete Random Walk (DRW) model. For the k-ε and k-ω based RANS models, the DRW model can be written as:

$$u_i' = \zeta_i \sqrt{2k/3} \tag{2.13}$$

where k is the turbulent kinetic energy and ζ_i is a normally distributed random number [20].

For the LES, most of the energy-containing eddies are solved. Compared with the solved turbulence, the unsolved (subgrid-scale) part is negligible for particle turbulence dispersion. Therefore, the filtered velocity field solved by the LES can be a good approximation to $\vec{u}$ in Equation (2.11) without the DRW model [12].

For the DES model, the solved flow field combines "LES-like" flow in the main stream, and "RANS-like" flow in the attached boundary layers. Therefore, the DRW model is needed only in the boundary layers. For the DES realizable k-ε model used in this study, the DRW model has the same form as Equation (2.13). Note that, in the LES region, the k represents the subgrid-scale turbulence kinetic energy, which is negligible. The DRW is then "switched off." In the RANS region, the k represents the total turbulence kinetic energy. The DRW model works in the RANS mode.

2.3. Combination of airflow and particle models

With the five airflow models (RANS, URANS, LES, DES1, and DES2) and two particle dispersion modeling approaches (Eulerian and Lagrangian methods), their combination can form ten different advanced models as follows:

- RANS + Eulerian (steady-state only)
- URANS + Eulerian
- LES + Eulerian
- DES1 + Eulerian
- DES2 + Eulerian
- RANS + Lagrangian (steady-state only)
- URANS + Lagrangian
- LES + Lagrangian
- DES1 + Lagrangian
- DES2 + Lagrangian

The following section will evaluate the performance of these ten models in predicting different airflow and particle dispersion in enclosed environments.

3. Evaluation of different airflow and particle dispersion models for enclosed environments

To evaluate the performance of the advanced models in predicting particle transport in enclosed environments, this investigation used a commercial CFD code, FLUENT 6.3, to calculate the airflow and particle distributions in two different rooms. The discretization used a second-order upwind scheme, except for the momentum equation for LES and DES, which used a bounded central difference scheme. The pressure equation used the PRESTO! scheme.

3.1. Particle dispersion in an isothermal clean room

The first study selected the experiment conducted by Murakami et al. [5]. They measured the airflow and particle concentration distributions in a ventilated clean room under isothermal conditions. Figure 1 depicts the configuration of the clean room. The air was supplied from two ceiling diffusers and exhausted from four outlets located at the lower walls of the room. The total air exchange rate was 40 ACH, corresponding to a flow rate of 0.64 m^3/s. The air velocity magnitude was measured by omni-directional anemometers and the direction was determined by monitoring a smoke tester. An optical particle counter was used to measure the particle concentration. Monodispersed polystyrene particles were generated by an atomizer. The particle concentration was about 6×10^8 particles/m^3 at the source. The particle size was 0.31 μm, and the density was 1050 kg/m^3. Since airborne particles of 0.3 μm in diameter have approximately the same diffusion properties as a gas [5], the gravitational force was not included in the settling velocity of the Eulerian method.

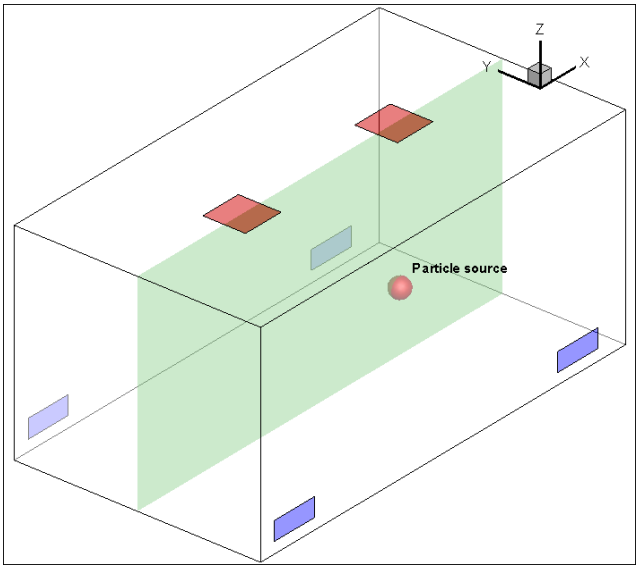

Figure 1 Schematic view of the clean room studied by Murakami et al. [5]. The measurement was performed on the green rectangle section

To check grid independence in CFD, three grid resolutions (14,000, 112,000, and 896,000) were tested for simulating the flow field. For such a simple flow, the 112,000 grid produced a reasonably good result compared with that of the 896,000 grid. Thus, the results with the 112,000 grid were used in this study and presented in this paper.

This study first simulated the airflow field in this room. Figure 2 compares the simulated airflow pattern using the RANS model with the measurement at the center plane of the room. The RANS model predicted corrected circulation pattern. However, only qualitative comparison can be made due to the accuracy of the measurement. Although not shown in this paper, this study also compared the results from other airflow models, and found that all the models predicted correct airflow pattern.

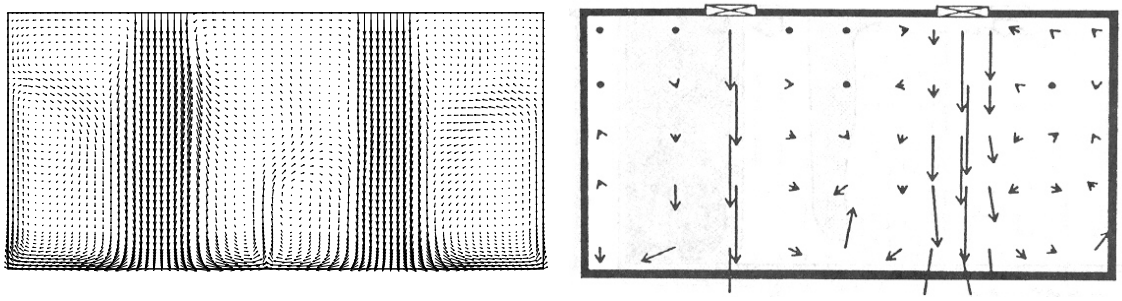

(a) Simulation (RANS) (b) measurement [5]

Figure 2 Comparison between the simulated and the measured airflow field: (a) simulated airflow field with RANS model, and (b) the measured airflow field.

Figure 3 compares the measured and simulated particle concentration distributions in the center plane of the room (the green plane in Figure 1). The results were normalized by the averaged particle concentration at the exhaust. The results from the RANS-Lagrangian model were calculated by the Particle Source in the Cell (PSI-C) method

based on a sample size (number of trajectories) of 100,000 [6]. The time step used by the unsteady airflow model was 0.01s. The unsteady airflow models with the Eulerian method were the averaged scalar concentration over five minutes. The results from the unsteady airflow models with Lagrangian methods were based on the averaged particle concentration over five minutes with 10,000 particles released per second.

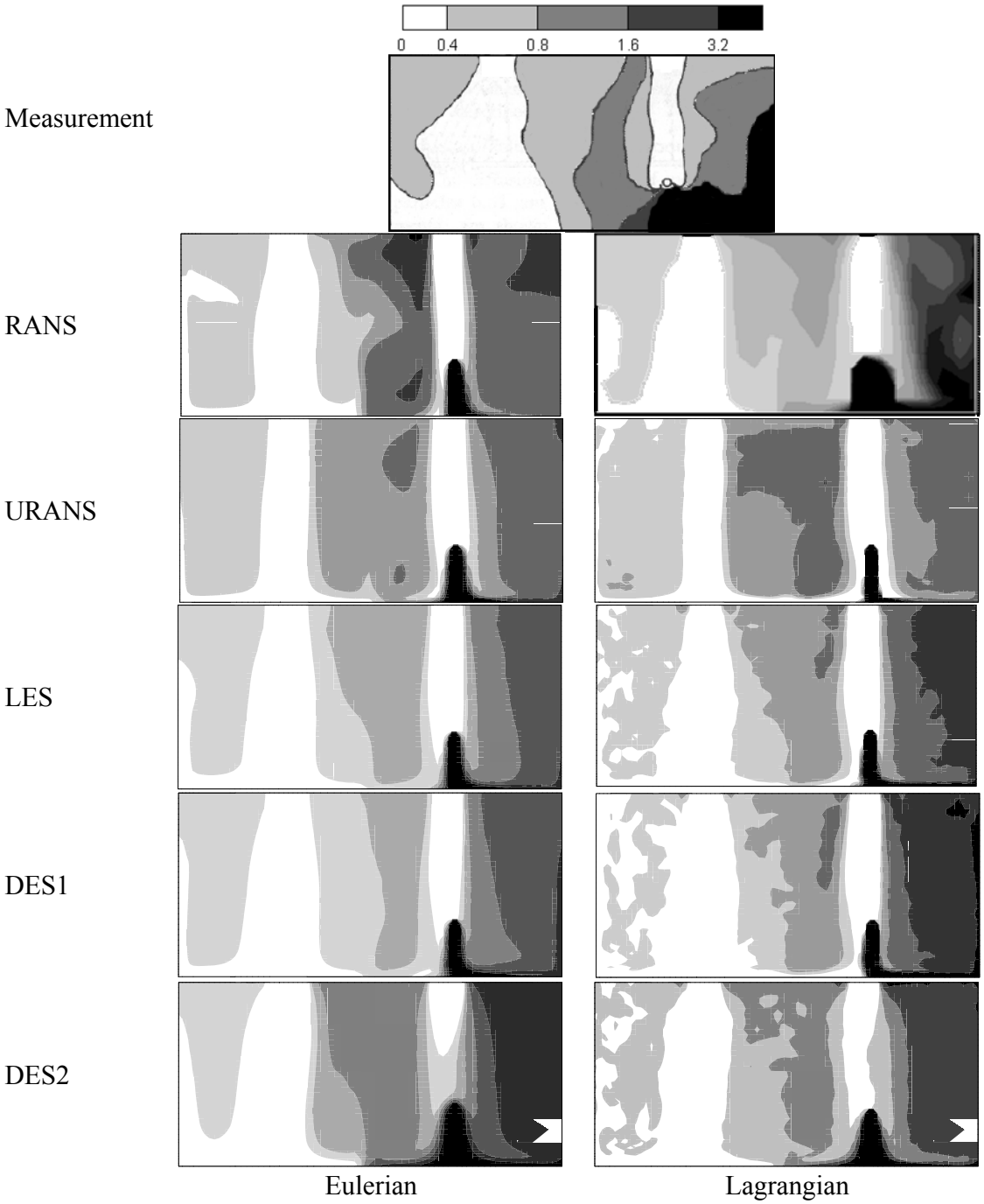

Figure 3 Comparison of the simulated particle-concentration distributions by the Eulerian and Lagrangian methods with the experimental data in the mid-section of the room.

All the airflow models with the Eulerian method predicted reasonable results, but failed to reproduce a high concentration zone at the lower-right corner. The performances of different airflow models were similar. This is because all the models shared the same scalar transport equation.

All the airflow models with the Lagrangian method predicted similar distributions except the URANS model, which predicted a larger high concentration zone on the left side of the room. The results from the Lagrangian method were more scattered than those from the Eulerian method due to its discrete nature. This phenomenon was also reported by several other studies [7, 10]. The results from the LES, DES1, and DES2 were even more scattered than those from RANS and URANS. This is understandable since the LES and DES models reproduced more unsteady eddy structures, which contributed to the turbulence dispersion of the particles. In contrast, the RANS and URANS used the isotropic DRW model to account for the turbulence dispersion, which led to a more diffusive particle concentration pattern.

3.2. Particle dispersion in a room with displacement ventilation

In the previous case, the ventilation rate was very high for an enclosed environment, and the case was isothermal. Therefore, this investigation chose a non-isothermal test case with a lower ventilation rate, as shown in Figure 3. The room had a UFAD system and four heated boxes simulating occupants. The air supplied from the two floor openings had a total flow rate of 0.0994 m^3/s, and it was exhausted from the ceiling. Monodispersed particles with a diameter of 0.7 μm were released into the room from a point source at 0.3 m above the floor. Note that indoor particles of this size are in the accumulation mode, which have low deposition rate [6]. Therefore, the particle deposition and gravitational sedimentation were neglected in the numerical simulation. The particle concentration was measured at six poles in the room, as shown in Figure 4. A more detailed description of the experiment and boundary conditions can be found in reference [6].

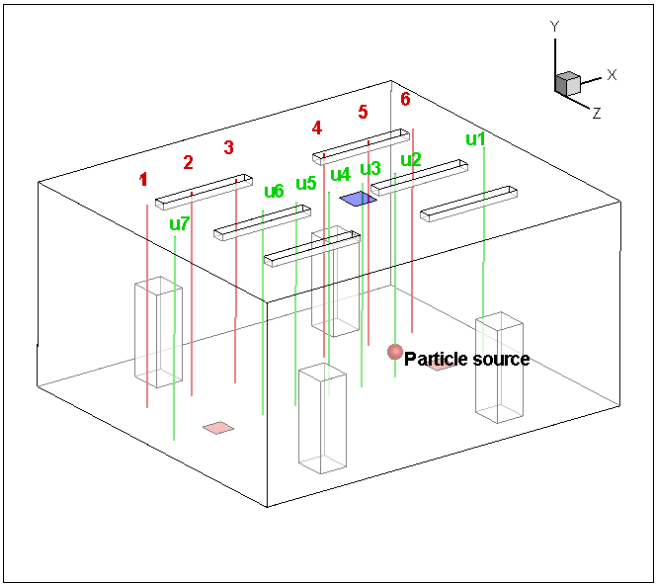

Figure 4 Schematic view of the non-isothermal room in which the particle concentration was measured at different heights along the six red lines, and air velocity was measured at the seven green lines

This CFD study again tested three grid resolutions (44,100, 352,100, and 1,630,000) to simulate the flow. The 352,100 grids generated similar results to those of the 1,630,000 grids; the results from the 352,100 grid are reported in this paper. The RANS-Lagrangian model used 500,000 trajectories. For the unsteady airflow models (URANS, LES, and DES1, and DES2) with the Lagrangian method, the particle generation rate was 1,000 particles per second. The transient concentration fields were averaged over ten minutes, corresponding to on complete air change. For the unsteady airflow models with the Eulerian method, the scalar concentration fields were also averaged over ten minutes. Again, the time step used in this case was 0.01s.

Figure 5 compares the simulated and measured air velocity at seven different poles (green lines in Figure 4). In general, the five turbulence models predicted comparable results for the air velocity, while the RANS model slightly over-predicted air velocity at the lower part of pole u1 and u2. At pole u7, all the five turbulence models over-predicted air velocity at lower part of the room.

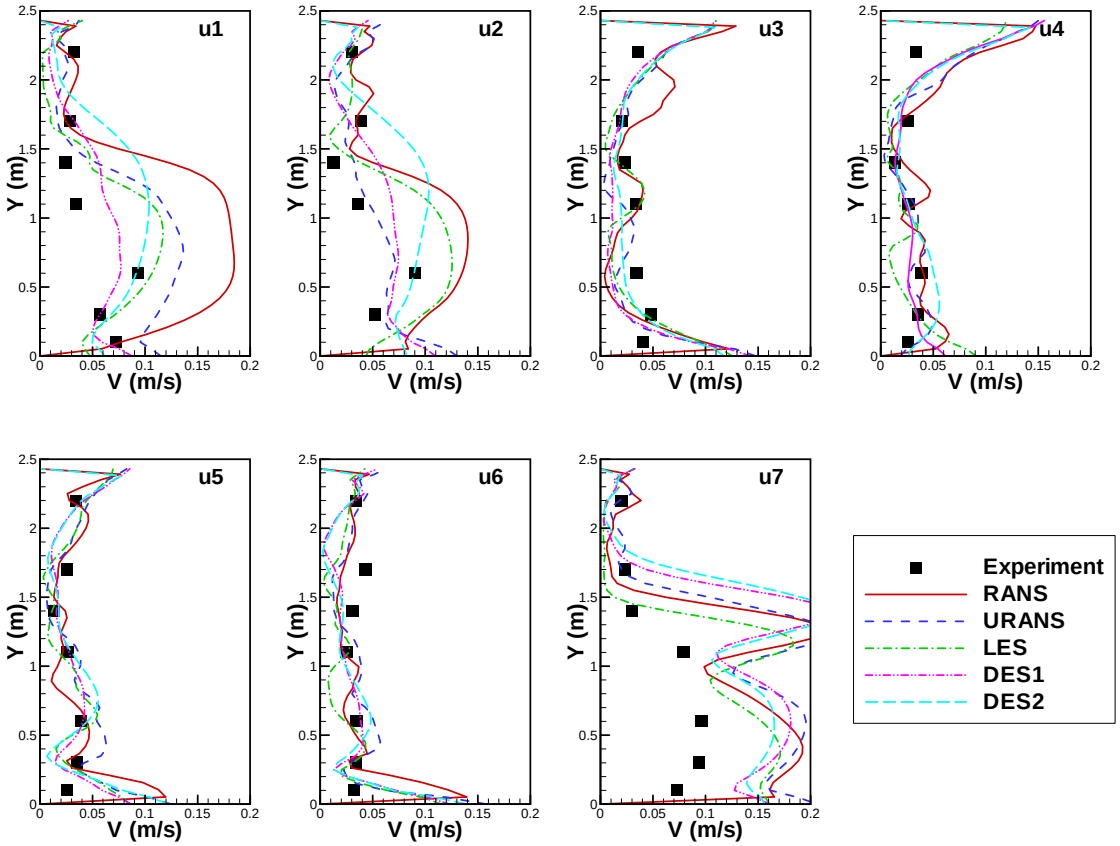

Figure 5 Comparison of the simulated and the measured air velocity at seven poles in the room with displacement ventilation.

Figure 6 compares the particle concentration profiles calculated by the five airflow models with the Eulerian method. As in the previous case, all the models predicted comparable results with correct magnitude. The URANS model over-predicted the concentration at the lower part of poles 2 and 3. The DES2 model under-predicted the concentration at the lower part of poles 3 and 4. The LES and two DES models predicted a straight profile at pole 5, while RANS and URANS predicted slightly better results. All the models predicted a straight profile at pole 6, where the experiment showed a higher concentration near the ceiling and floor than in the middle.

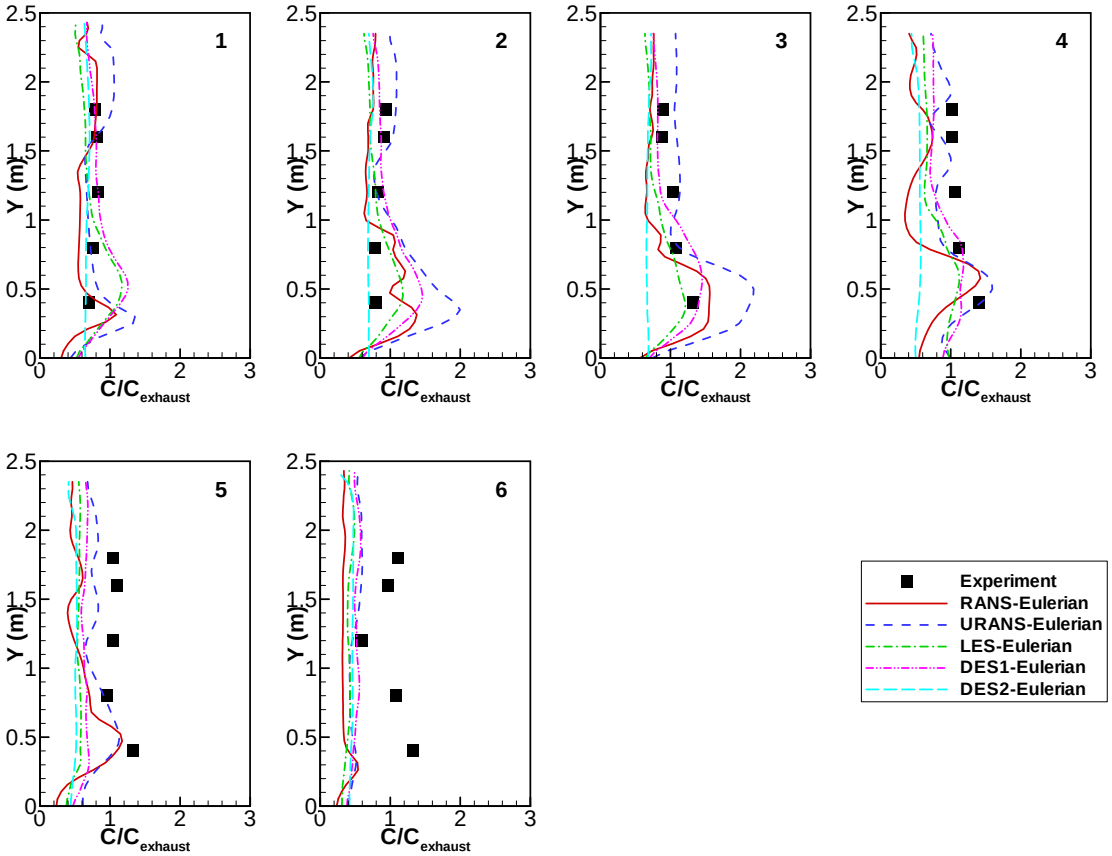

Figure 6 Comparison of the measured and calculated particle concentration profiles with the Eulerian method at the six poles in the room with displacement ventilation.

Figure 7 compares the particle concentration profiles calculated by the five airflow models with the Lagrangian method. Again, the results from the Lagrangian method were more scattered than those of the Eulerian method. Unlike the Eulerian method, the five models with the Lagrangian method showed a quite different performance. The URANS model and RANS model predicted large fluctuations at poles 2, 3, and 4. This was because, at these locations, the airflow driven by mechanical ventilation interacted with the thermal plumes, which generated an unstable separated flow. The RANS and URANS models could not perform well for such flow features [11]. In contrast, the LES and DES predicted more realistic profiles due to the better performance of an unstable flow.

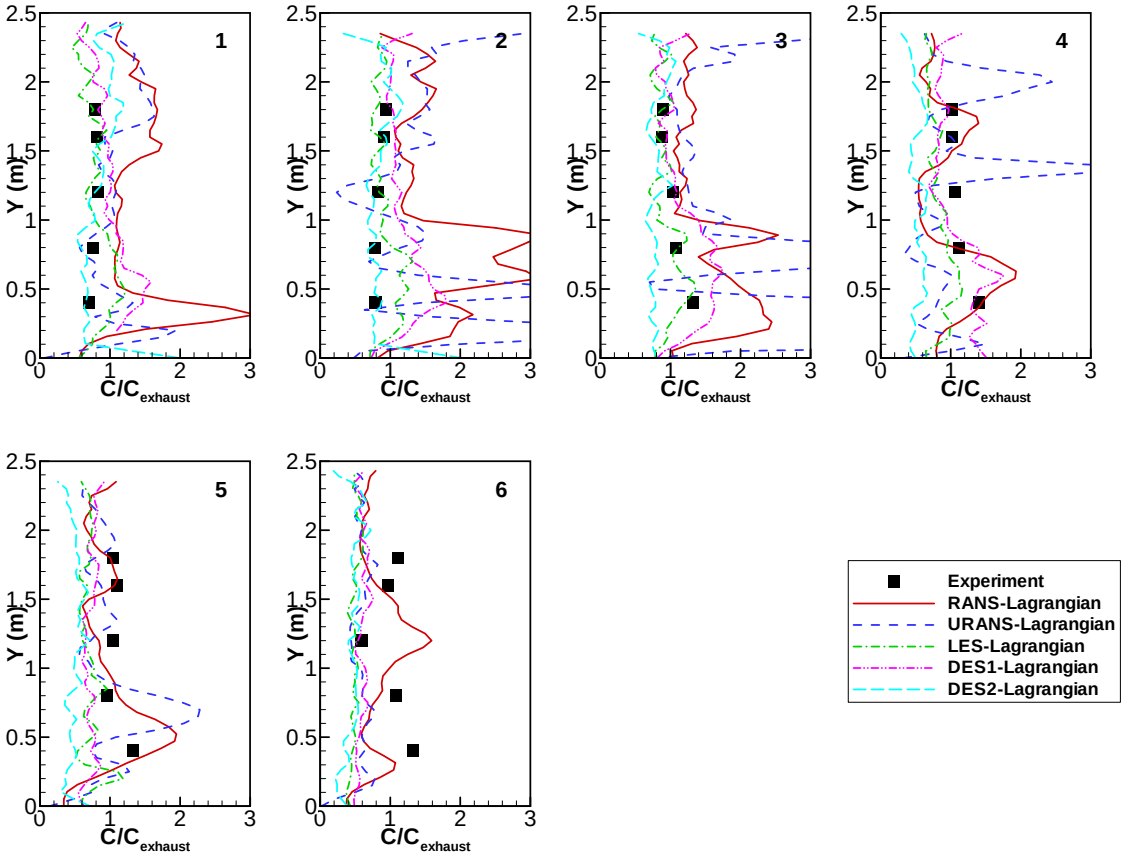

Figure 7 Comparison of the measured and calculated particle concentration profiles with the Lagrangian method at the six poles in the room with displacement ventilation.

3.3. Transient particle dispersion in a two-zone chamber

In the previous two cases, the contaminant source and the flow field were in steady state. The particle concentration field did not vary with time, which may not be the case in real enclosed environments. However, due to the complexity in measuring transient particle concentration, unsteady particle dispersion processes have not been well studied. Among the few transient particle dispersion experiments in the literature, the case measured by Lu et al. [24] was one of the best. As shown in Figure 8, a three-dimensional two-zone chamber was connected by a sliding door, which could be either fully open or closed. The ventilated air was supplied to the left zone (zone 1) through an opening located on the wall near the ceiling. In the right zone (zone 2), the air was exhausted from another opening near the floor. The air change rate was 10.26 ACH. The particle concentration was measured by an infra-red particle monitor at the center of each zone.

Initially, the sliding door was closed and the ventilation system was turned off. Particles of five size groups (1, 2, 3, 4 and 5 μm) were released into zone 1 and mixed with the room air until uniformly distributed. When the experiment began, the sliding door was opened, and the ventilation system was turned on. The particle concentrations at the center of each zone were measured every minute for a total of 26 minutes. In this case,

the rate of particle deposition was one order magnitude smaller than the particle extract by the ventilation system [24]. Therefore, this study neglected the influence of particle deposition.

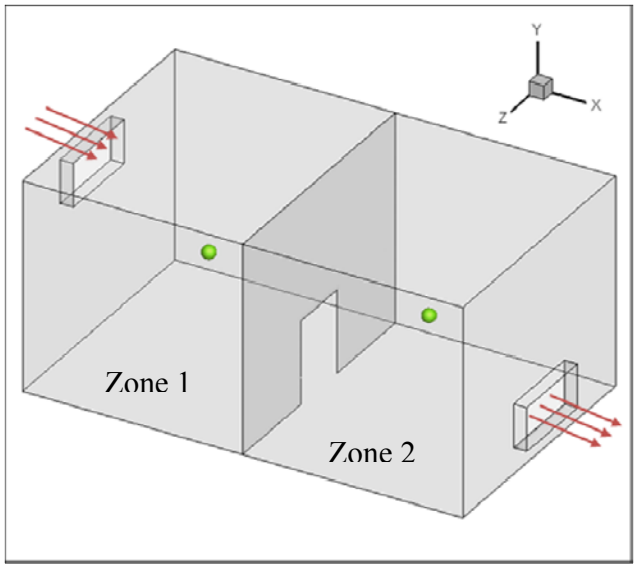

Figure 8 Schematic view of the two-zone chamber in which particle concentration was measured at the centers of the two zones.

Our investigation simulated this case from 0 to 26 minutes with a time step size of 0.01s. Three grid resolutions (26,600, 273,160, and 983,360) were tested for CFD grid independence. The 273,160 grid was sufficiently fine to capture such a flow and was used in particle tracking. Initially, one million particles were randomly located in zone 1, which was tested to be uniformly well distributed. Due to the unsteady nature of this case, only the transient solution was studied, and the steady RANS model was not used for this case. Note that the airflow field measurement was not available for this case. Therefore, the predicted airflow field was compared with the measurement.

Figure 9 shows the particle concentration evolution in the two zones predicted by different models. In zone 1 (Figure 9 (a) and (b)), the particle concentration decayed with time. The Eulerian model predicted decay profiles with too high concentration using the URANS model. This was because the URANS model could not capture the characters of the rapidly changing flow. The two particle models performed reasonably well with LES, DES1, and DES2 models, while the two DES models predicted slightly better results than did LES in terms of magnitude. For all flow models, the Lagrangian method predicted a small fluctuation after 15 minutes when the particle concentration was low. The Eulerian method predicted a smooth profile due to its scalar nature.

In zone 2 (Figure 9 (c) and (d)), again, the URANS model predicted incorrect results using both the Eulerian and Lagrangian methods. The LES, DES1, and DES2 models showed comparable performances. The Eulerian method predicted a larger fluctuation in the first six minutes, while the Lagrangian method predicted better results since it

accounted for more physics of flow and particle motion. After 20 minutes, all the models over-predicted the particle concentration, which was also reported by Lu et al. [24].

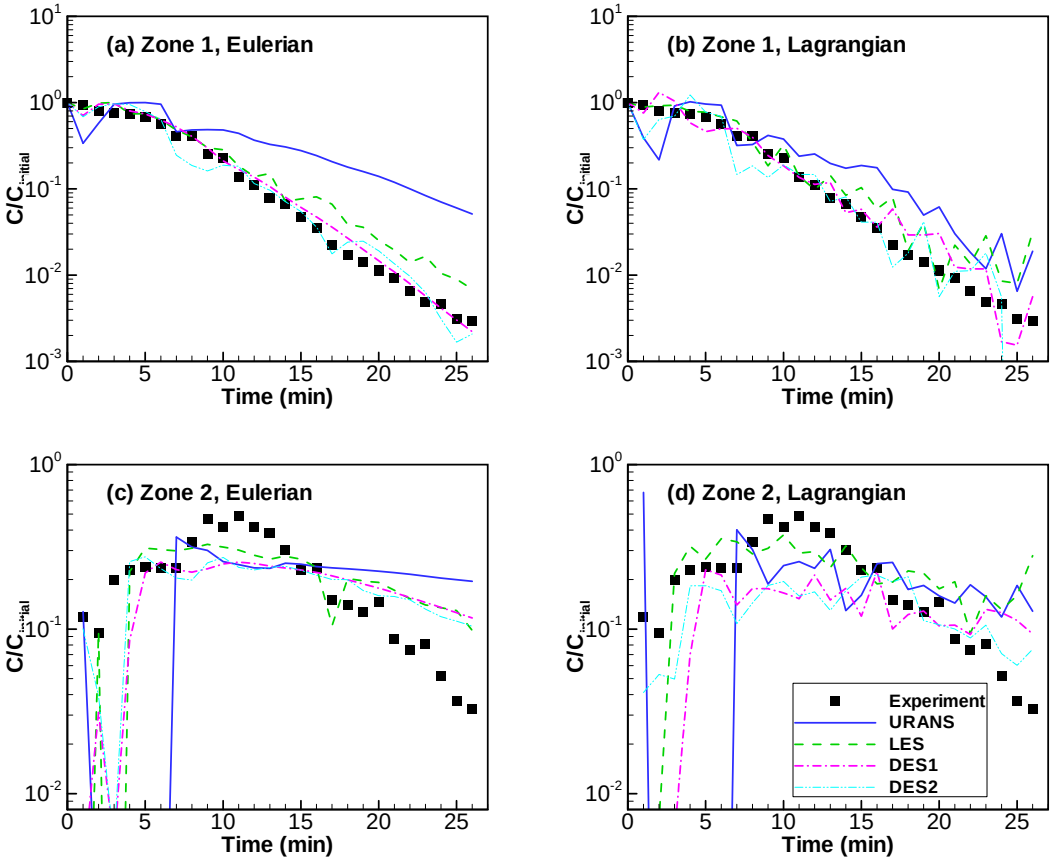

Figure 9 Comparison of the measured and predicted particle-concentration evolution in the two-zone chamber.

4. Discussion

While this investigation tested five airflow models with the Eulerian and Lagrangian methods for the three ventilation cases, it is of great interest to find out how to choose a model for a particular scenario. Table 1 summarizes the applicability and computing cost of each model. For the steady-state case, the Eulerian method can be applied with all five airflow models. The transport equation of the Eulerian method was identical for all airflow models. The resolved airflow was not the main factor in determining the particle distributions. For the Lagrangian method, the particle distribution pattern was primarily determined by the accuracy and richness of the flow structure resolved by the airflow model. Therefore, in many engineering flows with complex flow features, the isotropic RANS and URANS models tested in this study did not work well with the Lagrangian method. The performance may be improved if an anisotropic RANS model is applied. A LES or DES model is needed to provide well-resolved eddy structures for particle tracking.

Besides the accuracy, the computing cost is another important aspect in selecting models. For steady-state flows, the RANS model with the Eulerian method is the most cost efficient. However, if more detailed information is needed or particle dispersion is very complicated, such as chemical reaction, particle deposition, coagulation, and heat and mass transfer, the Lagrangian method should be used with a LES or DES model.

Table 1 Applicability and computing costs of different particle simulation models.

Method		Steady-state flows	Unsteady-state flows	Computing time (hour)*		
				Case 1	Case 2	Case 3
Eulerian	RANS	Yes	No	1.0	3.7	N/A
	URANS	Yes	No	15.4	74.2	62.2
	LES	Yes	No	28.8	75.0	323.3
	DES1	Yes	No	29.2	73.3	367.0
	DES2	Yes	No	34.1	98.3	396.6
Lagrangian	RANS	No	No	2.4	5.3	N/A
	URANS	No	No	17.9	81.5	84.9
	LES	Yes	Plausible	32.4	93.3	360.5
	DES1	Yes	Plausible	33.1	83.3	389.2
	DES2	Yes	Plausible	39.1	118.3	434.3

* The computing time was estimated on an eight-core cluster, with two 2.5GHz AMD quad-core processors and 32GB of memory.

For many unsteady-state cases, the URANS model failed to predict correct transient airflow [21]; thus, it should not be used. With the LES, DES1, and DES2 models, the Eulerian and Lagrangian methods showed a similar performance when the flow was in steady-state and the particle concentration field was in unsteady-state. However, when the flow field is still developing, the Lagrangian method may have better accuracy than the Eulerian method since it accounts for more physics of flow and particle motion. This conclusion is supported by Zhang and Chen [6], who simulated a cough case using both Eulerian and Lagrangian methods. They found that the Eulerian method generated unrealistic results.

5. Conclusions

This study compared the performance of five airflow models with the Eulerian and Lagrangian methods in predicting particle concentration distributions in enclosed environments. The five airflow models were a RANS model, a URANS model, a LES model, and two DES models. The study tested these models for two steady-state particle dispersion cases, a forced convection in a clean room and a mixed convection in a room with a UFAD system, as well as for an unsteady-state case, a ventilated two-zone chamber. The test results showed that the Eulerian method performed in a similar way for all five airflow models. The Lagrangian method predicted an incorrect particle concentration profile with the RANS and URANS models, but did well with the LES and DES models.

For steady-state cases, the RANS model with the Eulerian method is preferred for their reasonable accuracy and low computing cost. For unsteady-state cases, the LES or DES models with the Lagrangian method should be applied, in spite of the high computing cost. The Eulerian method may be improved if take into account more physics, such as gravitational force, Brownian motion and particle deposition.

Acknowledgements

This study was partially funded by the U.S. Federal Aviation Administration (FAA) Office of Aerospace Medicine through the National Air Transportation Center of Excellence for Research in the Intermodal Transport Environment at Purdue University under Cooperative Agreement 10-C-RITE-PU. Although FAA sponsored this project, it neither endorses nor rejects the findings of the research. This information is presented in the interest of invoking comments from the technical community about the results and conclusions of the research.

References

[1] EPA, Review of the national ambient air quality standards for particulate matter: Policy assessment of scientific and technical information, OAQPS Staff Paper; 2005.
[2] Moser MR, Bender TR, Margolis HS, Noble GR, Kendal AP, Ritter DG, An outbreak of influenza aboard a commercial airliner. Am J Epidemiol 1979; 110:1-6.
[3] Mangili A, Gendreau MA, Transmission of infectious disease during commercial air travel. Lancet 2005; 365:989-996.
[4] Han K, Zhu X, He F, Liu L, Zhang L, Ma H, Tang X, Huang T, Zeng G, Zhu BP, Lack of airborne transmission during outbreak of pandemic (H1N1) 2009 among tour group members. Emerg Infect Dis 2009;15:1578-81.
[5] Murakami S, Kato S, Nagano S, Tanaka S, Diffusion characteristics of airborne particles with gravitational settling in a convection-dominant indoor flow field. ASHRAE Transactions 1992; 98 (part 1), 82–97.
[6] Zhang Z, Chen Q, Experimental measurements and numerical simulations of particle transport and distribution in ventilated rooms. Atmospheric Environment 2006;40(18):3396-3408.
[7] Zhang Z, Chen X, Mazumdar S, Zhang T, Chen Q, Experimental and numerical investigation of airflow and contaminant transport in an airliner cabin mockup. Building and Environment 2009; 44(1):85-94.
[8] Yin Y, Xu W, Gupta JK, Guity A, Marmion P, Manning A, Gulick RW, Zhang X, Chen Q. Experimental study on displacement and mixing ventilation systems for a patient ward. HVAC&R Research 2009; 15(6):1175-1191.
[9] Zhai ZQ, Zhang W, Zhang Z, Chen Q. Evaluation of various turbulence models in predicting airflow and turbulence in enclosed environments by CFD: part 1 - Summary of prevalent turbulence models. HVAC&R Research 2007; 13(6):853-870.
[10] Zhang Z, Zhai ZQ, Zhang W, Chen Q. Evaluation of various turbulence models in predicting airflow and turbulence in enclosed environments by CFD: Part 2-comparison with experimental data from literature. HVAC&R Research 2007; 13(6):871-886.

[11] Wang M, Chen Q, Assessment of various turbulence models for transitional flows in enclosed environment. HVAC&R Research 2009; 15(6):1099-1119.
[12] Béghein C, Jiang Y, Chen Q. Using large eddy simulation to study particle motions in a room. Indoor Air 2005; 15(4):281-290.
[13] Lin CH, Wu TT, Horstman RH, Lebbin PA, Hosni MH, Jones BW, Beck BT. Comparison of large eddy simulation predictions with particle image velocimetry data for the airflow in a generic cabin model. HVAC&R Research 2006; 12(3c):935-951.
[14] Hasamaa T, Kato S, Ooka R, Analysis of wind-induced inflow and outflow through a single opening using LES & DES. Journal of Wind Engineering and Industrial Aerodynamics 2008; 96(10-11):1678-1691.
[15] Yakhot V, Orszag SA, Renormalization group analysis of turbulence. Journal of Scientific Computing 1986; 1:3-51.
[16] Suzuki Y, Mazumdar S, Kondo Y, Yoshino H, Chen Q, Effect of a moving object on air and contaminant distributions in a commercial kitchen with electrical cooking appliances. Proceedings of the 11th International Conference on Air Distribution in Rooms (ROOMVENT 2009), Busan, Korea.
[17] Mazumdar S, Yin Y, Guity A, Marmion P, Gulick B, Chen Q, Impact of moving objects on contaminant concentration distributions in an inpatient room with displacement ventilation. HVAC&R Research 2010; 16(5), 545-564.
[18] Germano M, Piomelli U, Moin P, Cabot WH, Dynamic subgrid-scale eddy viscosity model. In Summer Workshop 1996; Center for Turbulence Research, Stanford, CA; 1996.
[19] Lilly DK, A proposed modification of the Germano Subgrid-Scale Closure Model. Physics of Fluids 1992; 4:633-635.
[20] FLUENT, FLUENT 6.3 Documentation, Fluent Inc., Lebanon, NH; 2006.
[21] Wang M, Chen Q, On a hybrid RANS/LES approach for indoor airflow modeling. HVAC&R Research 2010; 16(6), 731-747.
[22] Hinze JO, Turbulence, 2nd Edition, New York: McGraw-Hill; 1975;460 – 471.
[23] Lai ACK, Nazaroff WW, Modeling indoor particle deposition from turbulent flow onto smooth surfaces. Journal of Aerosol Science 2000; 31(4):463 - 476.
[24] Lu W, Howarth AT, Adam N, Riffa SB, Modelling and measurement of airflow and aerosol particle distribution in a ventilated two-zone chamber. Building and Environment 1996; 31(5,):417-423.